IMPACT OF THE SURFACE ENHANCEMENT ON THE HEAT TRANSFER IN A MINICHANNEL

Piasecka M.* and Strąk K.
*Author for correspondence
Department of Mechatronics and Mechanical Engineering
Kielce University of Technology,
Al. 1000-lecia P.P. 7, 25-314 Kielce
Poland
E-mail: tmpmj@tu.kielce.pl

ABSTRACT

This paper presents results concerning flow boiling heat transfer in three parallel vertically oriented and asymmetrically heated rectangular minichannels. Each minichannel was 1.7 mm deep, 16 mm wide and 180 mm long. The heated element for Fluorinert FC-72 flowing in the minichannels was a thin alloy foil. Infrared thermography was used to determine changes in the temperature on the outer smooth side of the foil. Two-phase flow patterns were observed through a glass pane. The heated surfaces in contact with the fluid in the minichannels differed in roughness. In one minichannel the heated surface was smooth. In the other two, the heated surface was enhanced. Two types of surface enhancement were analyzed: a surface with unevenly distributed minicavities and a surface coated with metallic powder applied by soldering. This paper analyzes the effects of the microstructured heated surface on the heat transfer coefficient. The results are presented as relationships between the heat transfer coefficient and the distance along the minichannel length and as boiling curves. The experimental data obtained for the two types of enhanced heated surfaces was compared with the results recorded for the smooth heated surface. The highest local values of the heat transfer coefficient were reported for the enhanced foil with minicavities.

INTRODUCTION

Recently, research on heat transfer has focused on phenomena occurring in minichannels so that the solutions can be used in cooling systems for electronic devices. The aim of the investigations is to produce highest possible heat fluxes while keeping a small difference in temperature between the heated surface and the saturated liquid. Flow boiling heat transfer in small-size systems can be improved by applying enhanced or porous surfaces. This has been confirmed for pool boiling. From the experimental results concerning flow boiling heat transfer obtained by different researchers it is evident that the process can be intensified by using enhanced surfaces.

Many studies have been conducted on heat transfer with phase change in micro- and minichannels [1-10] over the last twenty years, but there are very few papers pertaining to flow boiling heat transfer in minichannels with enhanced heated surfaces. Reference [11] discusses the performance of three different minichannel heat exchangers (MCHEs) of an automotive air-conditioning system. The results concerning the glycol-water flow in the minichannels indicate that the Nusselt number increased with the Reynolds number because of the use of unique surface enhancements − louvered thin-plate fins. Reference [12] is a comprehensive study of flow and pool nucleate boiling of pure refrigerants R22, R134a, and R407C on enhanced surfaces. Three types of surfaces were analyzed: flat circular plates and horizontal tubes coated with a porous layer, a single horizontal tube partially coated with a porous layer and a bundle of horizontal tubes coated with a porous layer. The average heat transfer coefficient reported for porous surfaces was five to six times higher than that obtained for a smooth surface (stainless-steel tubes); the pressure drop, however, was lower. Reference [13] deals with the enhancement of convective boiling heat transfer in a small channel achieved by applying a microporous coating. The influence of surface roughness on flow boiling heat transfer in microchannels was analyzed also in Ref. [14]. The study reveals that surface roughness can have a considerable effect on the heat transfer coefficient and the pressure drop but it does not seem to significantly affect the boiling incipience wall temperature.

NOMENCLATURE

A	[m^2]	Surface area
I	[A]	Current supplied to the heated foil
q_w	[W/m^2]	Heat flux density
q_{loss}	[W/m^2]	Loss of the heat flux to the surroundings
T	[K]	Temperature
T_s	[K]	Ambient temperature
x	[m]	Distance from the minichannel inlet

Special characters

α	[W/(m^{2}K)]	Heat transfer coefficient
α_s	[W/(m^{2}K)]	Heat transfer coefficient at the interface between the heated foil and the surroundings
ΔU	[V]	Voltage drop
δ	[m]	Thickness

Subscripts

F	Foil
f	Fluid
l	Liquid
s	Surroundings
sat	Saturation

In their earlier research [15-22], the authors studied flow boiling heat transfer in minichannels where the cooling fluid was heated by an enhanced surface. Liquid crystal thermography and infrared thermography were applied to measure the temperature of the heated element. Local values of the heat transfer coefficient were calculated numerically using one- and two-dimensional models.

Many research reports include boiling curves to illustrate the differences in parameters, boiling regions, working fluids, etc. In Ref. [23] the boiling curves were generated for the saturated boiling region and the subcooling boiling region. The boiling curve can also be used to analyze the behaviour of various working fluids, for example, FC-72 in mini circular tubes [24] or FC-72 and distilled water [25] under normal and low gravity conditions [26]. In Ref. [12], the boiling curves were plotted for different porous surfaces; they show that the heat transfer coefficient was higher for a bundle of tubes coated with a porous layer than for a bundle of smooth tubes, irrespective of the liquid used, the pitch-to diameter ratio or the operating pressure.

This paper discusses the influence of a microstructured surface on the heat transfer coefficient in flow boiling heat transfer for FC-72 flowing in three asymmetrically heated parallel vertical minichannels. Infrared thermography was used to observe changes in the temperature on the outer smooth side of the foil. The heated surfaces in contact with the fluid in the minichannels differed in roughness. The results are presented as relationships between the heat transfer coefficient and the distance along the minichannel length and as boiling curves.

EXPERIMENT

The experimental stand with main loops and a data acquisition system is represented schematically in Fig. 1a. The flow loop comprises a test section (1), a rotary pump (2), a compensating tank (3), a heat exchanger (4), a filter (5), mass flowmeter (6), a deaerator (7) and pressure converters (8). The data and image acquisition systems with an infrared camera (9) and a digital SLR camera (10), a lighting system (11), a data acquisition station (12) and a computer with specialized software (13) are the essential parts of the research equipment. The supply and control system consists of a inverter welder (14), a shunt (15), an ammeter (16) and a voltmeter (17).

The test module with three parallel vertically oriented minichannels, each 1.7 mm deep, 16 mm wide and 180 mm long (Fig. 1b), is the most important part of the experimental stand. The heated element for FC-72 flowing in the minichannels (25) is the 0.1 mm thick foil made of Haynes-230 alloy (18). One minichannel had a smooth heated surface contacting fluid, in the other two, the heated surface was rough (19). The roughness was achieved either by producing unevenly distributed minicavities or applying iron powder by means of soldering. The outer smooth side of the heated foil of each minichannel was strengthened on both sides with narrow micanite panels to prevent the foil surface from deforming. An *FLIR* infrared camera (9, Fig. 1a) positioned opposite the central, axially symmetric part of the channel measured the foil temperature. The surface of the foil was coated with black paint (24, Fig. 1b) of a known emissivity (about 0.83) [27]. The two-phase flow patterns on the foil surface in contact with the fluid in the minichannels were observed through a glass pane (20, Fig. 1b) using Canon EOS 550D digital SLR camera (10, Fig. 1a) and illuminated by high power LEDs (11). K-type thermocouples (23, Fig. 1b) and pressure converters (8, Fig. 1a) were installed at the inlet and outlet of the minichannel.

The accuracy of the E60 *FLIR* infrared camera was ± 1 °C or ± 1% in the temperature range: 0 ÷ 120 °C. The mean error calculated for the foil temperature measured under laboratory conditions using predefined camera settings was 0.7 K. This result constitutes 1% of the experimental temperature range. The error for the fluid temperature was calculated as an error of temperature from the thermoelements placed at the inlet and outlet of the minichannels. This error includes errors resulting from signal processing by the acquisition cards in the measurement data acquisition station and the thermocouple sensor errors. It was estimated to be 0.77 K [28-29]. The maximum error for the mass flow measured with a Promass 80A04 mass flowmeter (Endress+Hauser), constituted 0.15% of the full scale reading and it was estimated to be 0.675 kg/h. The pressure of the fluid at the inlet and outlet of the minichannels was measured using Endress+Hauser PMP51 Cerabar M pressure converters. The value registered with an accuracy of ± 0.05% of the full scale was 5·10-3 bar.

The core information on the physical properties of FC-72 was quoted from Ref. [30], where it was presented in the form of polynomial equations. More detailed data was obtained from the REFPROP program.

The heated foil was made of Haynes 230 superalloy produced by US-based Haynes International, Inc. The alloy constituents include Ni, Cr, W and Mo. The foil has a guaranteed precision thickness of 0.004" (approx. 0.1 mm). After the length and width of the heated foil were measured with a vernier caliper, the absolute errors were estimated. They were $5 \cdot 10^{-5}$ m.

In each minichannel, the heated surface had a different texture: one surface was smooth and the other two were rough.

- The smooth surface of the first minichannel was made of Haynes-230, 0.1 mm thick acid-proof rolled plate with the surface roughness being Ra = 0.121 μm [19, 31].
- The microstructured surface in the next minichannel was enhanced by electrical discharge machining (spark erosion), using an electric-etcher and a manually controlled branding-pen. Typical cavities produced with this technique can be seen in Fig. 1c. The average depth of the cavities was below 1 μm. The rims of the resolidified melt from the electrode and the foil were up to 5 μm in height, [19, 21].
- The microstructured surface in the last minichannel was produced by soldering iron powder to the Haynes-230 alloy foil (Fig. 1d). The main parameters of the microstructured surface are: the diameter of a solder granule - approx. 15÷80 μm (with an average being 40÷65 μm); the density of the solder paste – 2990 kg/m^3, the thickness of the soldered layer – approx. 100 μm; the maximum height of the soldered layer – 200 μm.

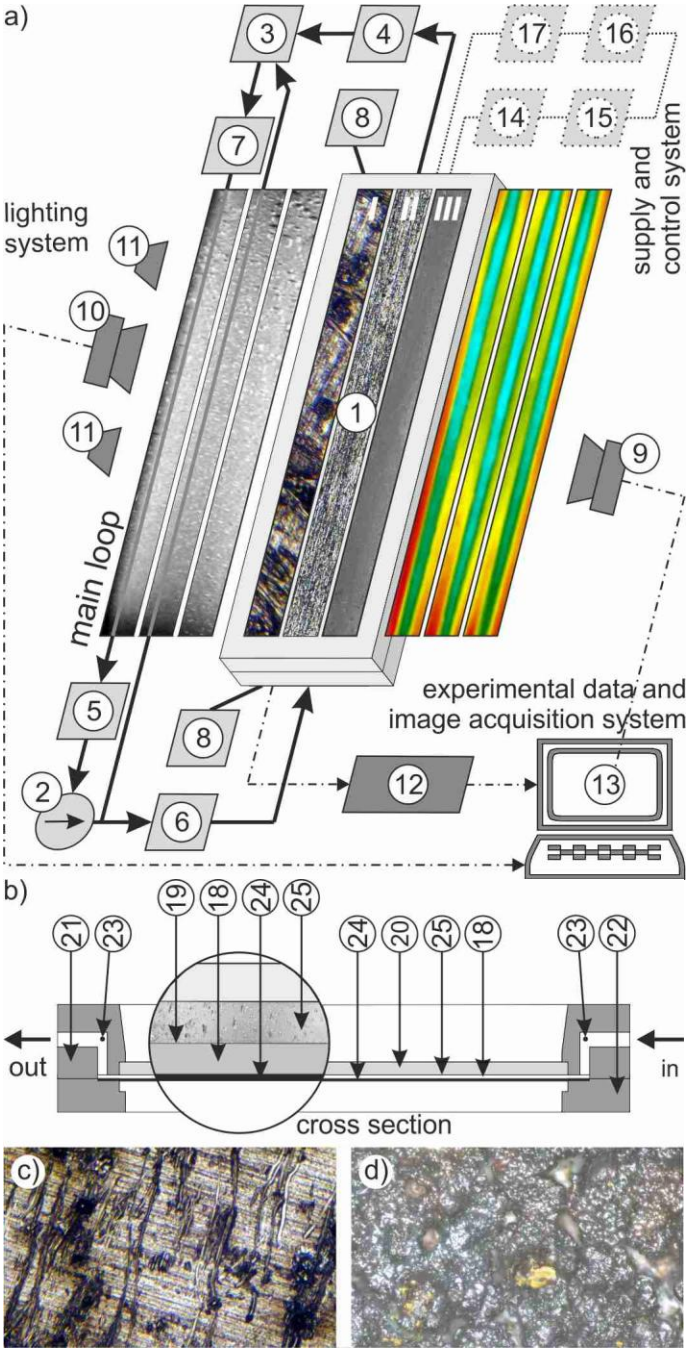

Figure 1 Schematic diagrams of: a) the main loops and the data acquisition system at the experimental setup, 1-test section with minichannels; 2-rotary pump; 3-compensating tank; 4-tube-type heat exchanger, 5-filter, 6-mass flowmeter, 7-deaerator, 8-pressure converter, 9-infrared camera; 10-digital SLR camera, 11-high power LEDs, 12-data acquisition station, 13-computer, 14-inverter welder, 15-shunt, 16-ammeter, 17-voltmeter; b) the test module with minichannels: 18-heated foil, 19- smooth or enhanced surface of the foil, 20-glass pane, 21-channel body, 22-front cover, 23-thermocouple,24-black paint layer, 25-minichannel; c, d) images of a fragment of the foil surface enhanced by electrical discharge machining (c) and soldering of iron powder (d)

An experimental series was performed to study the laminar flow of Fluorinert FC-72 in three parallel asymmetrically heated minichannels. After the desired values of the pressure and flow rate were reached, the electric power supplied to the heated element was increased gradually to achieve an increase in the heat flux transferred to the fluid in the channel. The increase in the heat flux caused a change in the heat transfer between the foil and the working fluid in the minichannels from single phase convection to nucleate boiling. The process began with the onset of nucleate boiling and subcooled boiling. In the subcooled boiling region, the liquid was superheated at the interface with the foil and subcooled at the core of the flow. Saturated nucleate boiling occurred when the fluid reached its saturation temperature at the core of the flow.

The distribution of temperature on the heated foil was measured on the smooth side coated with a black paint layer. Simultaneous observations of the flow structure were conducted on the opposite side of the minichannel.

HEAT TRANSFER COEFFICIENT DETERMINATION

The local heat transfer coefficients will be presented and discussed separately for two boiling regions: the saturated boiling region and the subcooled boiling region.

The local values of the heat transfer coefficient were calculated using simple one-dimensional method which take into account the heat flow direction perpendicular to the direction of the fluid flow in the minichannel [18]. The resulting local heat transfer coefficients $\alpha(x)$ were obtained from the following equation:

$$\alpha(x) = \frac{q_w(x)}{T_F(x,\delta) - T_f(x)} \tag{1}$$

where x − distance from the minichannel inlet, T_F − foil temperature measured by infrared thermography, δ – thickness of the heated foil, T_f – temperature of the fluid, assuming that $T_f = T_l$ in the subcooled boiling region and $T_f = T_{sat}$ in the saturated nucleate boiling region, T_l – fluid temperature calculated from the assumption of the linear distribution of the fluid temperature along the minichannels, T_{sat} – saturation temperature determined from the assumption of the linear distribution of the fluid pressure along the minichannels.

The heat transferred to the fluid in the minichannel was assumed to be equal to the difference between the heat generated by the heating foil and the heat loss to the surroundings:

$$q_w = \frac{I \cdot \Delta U}{A} - q_{wloss} \tag{2}$$

where q_w − heat flux proportional to the surface area of the heating foil in each minichannel, I - current, ΔU - voltage drop, A - surface area of the heated foil in the minichannel proportional to the for each minichannel, q_{wloss} − heat loss to the surroundings.

The central part of the heating foil where the surface temperature is measured with the infrared camera (4 mm x 180 mm) is not insulated for each minichannel. Therefore, the loss of heat to the surroundings is the greatest.

It was estimated as 1.3% of the heat flux density [18], according to formula:

$$q_{wloss} = \alpha_s \cdot [(T_F\ (x,\delta) - T_s] \quad (3)$$

where α_s − local values of the heat transfer coefficient at the interface between the heated foil and the surroundings, and T_s − ambient temperature.

The loss was relatively small because the measurement module itself was quite small.

The average uncertainties of the relative heat transfer coefficient and the heat flux density were calculated in accordance with the principles of measurement accuracy analysis, in the same way as in [29]. The results of the error analysis are provided in Table 1, separately for the subcooled and saturated boiling regions, with errors specified for each setting of the heat flux density.

Table 1 The average uncertainties of the relative heat transfer coefficient and the heat flux density

Subcooled boiling region			Saturated boiling region		
Set of heat flux (No.)	Average uncertainties		Set of heat flux (No.)	Average uncertainties	
	q_w	α		q_w	α
1	10.49	16.54	5	6.89	59.98
2	9.31	19.80	6	6.47	59.60
3	8.83	15.83	7	6.10	54.47
4	7.21	11.00	8	5.50	44.66

The mean errors of the heat transfer coefficient differed considerably between the boiling regions. The lowest values were obtained in the subcooled boiling region (up to 20%) and the highest in the saturated boiling region (up to 60%). However, the average error of the heat transfer coefficient for either boiling region was approximately 35%.

RESULTS

The results are represented graphically as a relationship between the heat transfer coefficient and the distance from the minichannel inlet to compare the heat transfer on the enhanced foil (textures produced by electrical discharge machining or by soldering of iron powder) with that on the smooth foil. Separate plots were generated for the subcooled boiling region (Fig. 2) and the saturated boiling region (Fig. 3). The values of the heat transfer coefficient calculated for the smooth surface, the enhanced surface produced by electrical discharge machining and the enhanced surface produced by soldering iron powder were marked as red points, green points and blue points, respectively. The temperatures of the heating surface at the inlet and outlet of each minichannel (about 10% from each side) were ignored due to the occurrence of the largest measurement errors when using IR thermography, as reported in detail in [31].

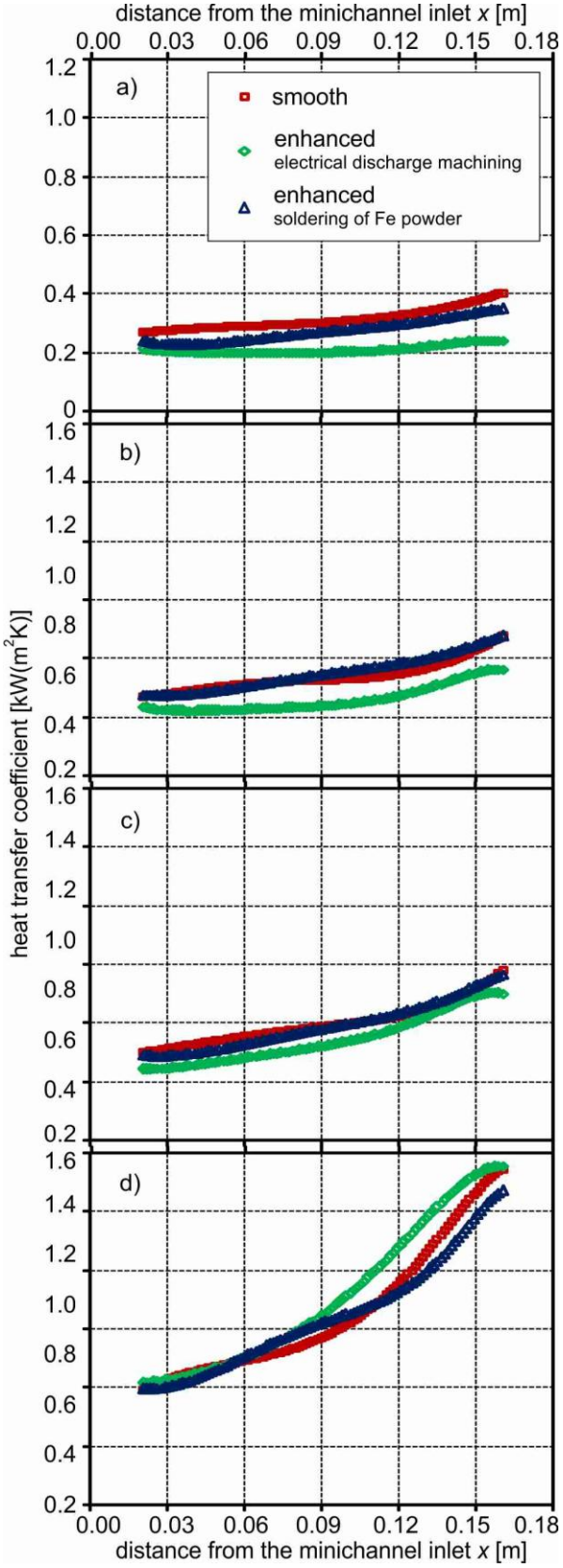

Figure 2 Heat transfer coefficient vs. the minichannel length; data for the subcooled boiling region; experimental parameters shown in Table 2, set of heat flux No.: a) 1, b) 2, c) 3, d) 4

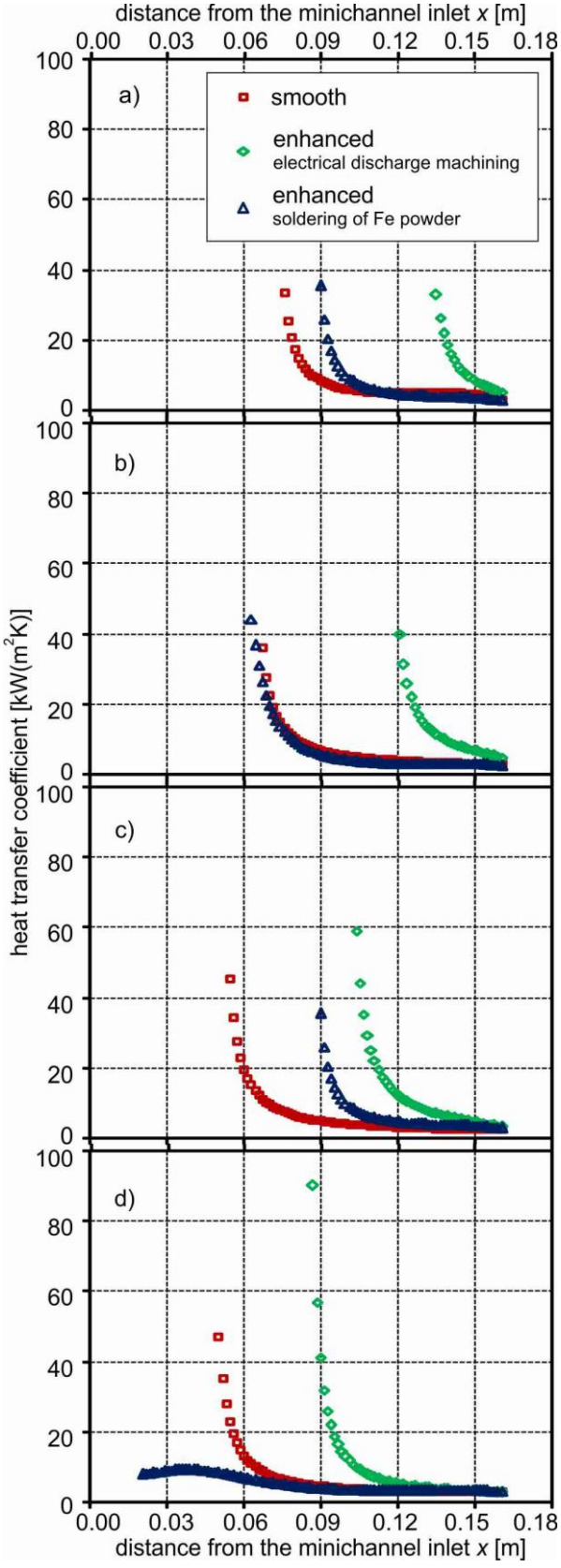

Figure 3 Heat transfer coefficient vs. the minichannel length; data for the saturated boiling region, experimental parameters shown in Table 3, set of heat flux No.: a) 5, b) 6, c) 7, d) 8

The experimental parameters for the subcooled and saturated boiling regions are presented in Tables 2 and 3, respectively.

Table 2 Experimental parameters for the subcooled boiling region

Set of heat flux (No.)	Average mass flux G [kg/(m^{2}s)]	Average inlet pressure p_{in} [kPa]	Average inlet liquid subcooling ΔT_{sub} [K]	Heat flux density q_w [kW/m^2]
1	417	119	42.6	6.647
2				8.446
3				9.397
4				14.278

Table 3 Experimental parameters for the saturated boiling region

Heat flux	Average mass flux G [kg/(m^{2}s)]	Average inlet pressure p_{in} [kPa]	Average inlet liquid subcooling ΔT_{sub} [K]	Heat flux density q_w [kW/m^2]
5	402	160	47.5	15.639
6				17.824
7				20.213
8				22.929

In the subcooled boiling region, the heat transfer coefficient was relatively low. The local values of the heat transfer coefficient increased slightly with the distance from the minichannel inlet (Fig. 2). At the lowest heat flux supplied to the foil, the local values of the heat transfer coefficient were the lowest for the surface enhanced by electrical discharge machining and the highest for the smooth surface (Fig. 2a). However, when the heat flux was the highest, the heat transfer coefficient was reported to be the highest for the surface modified by electrical discharge machining at the minichannel outlet (Fig. 2d). In the analyzed boiling region, the data obtained for the surface enhanced by soldering iron powder did not differ significantly from that reported for the smooth surface.

The analysis of the data presented in Fig. 3 indicates that the transition from the subcooled to the saturated boiling region occurred at about 1/3 of the distance from the minichannel inlet. It was possible to calculate the heat transfer coefficient when the coolant temperature reached saturation temperature in the saturated boiling region. In this region, the heat transfer coefficient was very high for all the heated surfaces, with values up to a hundred times greater than those obtained for the subcooled boiling region. In the saturated boiling region, the heat transfer coefficient decreased substantially with an increase in the distance from the minichannel inlet. That was due to an increase in the vapour volume fraction in the two-phase flow mixture [17-20]. The lowest values of the coefficient were observed at the channel outlet. When the heat

flux supplied to the foil was the lowest (Fig. 3a), the local values of the heat transfer coefficient were similar for all the tested surfaces reaching a maximum of 40 kW/(m^{2}K). Saturated boiling began close to the minichannel outlet; it then moved toward the channel inlet with increasing heat flux for the smooth surface and that modified by electrical discharge machining. The data obtained for the surface enhanced by soldering iron powder shows different distances for the onset of saturated boiling and a considerable decrease in the local values of the heat transfer coefficient at the highest heat flux (Fig. 4d). The slight porosity of the powder-based iron structure was responsible for locally high values of thermal resistance at diffusion bridges, a decrease in the surface wettability during fluid flow, and the generation of vapour plugs contributing to a reduction in the heat transfer efficiency. However, when the heat flux supplied to the foil increased (Fig 3c-d), the values of the heat transfer coefficient were much higher, reaching about 90 kW/(m^{2}K), for the surface with unevenly distributed minicavities rather than for the other surfaces. It is thus evident that heat transfer reported for this surface was more intensive than for the other heated surfaces.

Boiling curves were drawn from the data collected during tests, which involved first increasing and then decreasing the heat flux supplied to the heated surface. Boiling curves are usually plotted for selected points in the channel, corresponding to predetermined distances from the inlet, where the heat flux density depends on the surface superheating. Moreover, boiling curves frequently represent the relationship between the heat flux density and the difference in temperature between the heated surface and the bulk fluid in the case of flow boiling in minichannels. Such boiling curves are very useful because they show the subcooled boiling region data.

The boiling curves in Fig. 4 were generated for three distances from the minichannel inlet: 0.06 m, 0.105 m and 0.15 m. They were plotted as the heat flux density against the difference T_F-T_f. The boiling curves drawn for the two enhanced surfaces, i.e. one with cavities produced by electrical discharge machining and the other with cavities obtained by soldering iron powder, were compared with the boiling curve created for the smooth surface.

The boiling curves plotted for flow boiling heat transfer in the minichannel with the surface enhanced by electrical discharge machining were typical in shape (Fig. 4, green points). The analysis of the boiling curve marked in green in Fig. 4b shows that an increase in the heat flux density (from point A to point BI - nucleate boiling incipience) results in the single phase forced convection transfer of heat between the heated surface and the subcooled liquid in the minichannel. In the area adjacent to the foil, the liquid becomes superheated, whereas in the flow core it remains subcooled. An increase in the heat flux density leads to the activation of vapour nuclei on the heated surface. Spontaneous nucleation causes a drop in the temperature of the heated surface, as observed between point BI and point C. The bubbles act as internal heat sinks, absorbing a significant amount of energy transferred to the liquid [32-33]. This "temperature overshoot" also referred to as "superheated excursion" or "nucleation hysteresis" is characteristic of highly wetting dielectric fluids (e.g. refrigerants). The nucleation hysteresis is strongly dependent on the local distribution of nucleation sites and the wetting characteristics of the flowing cooling liquids.

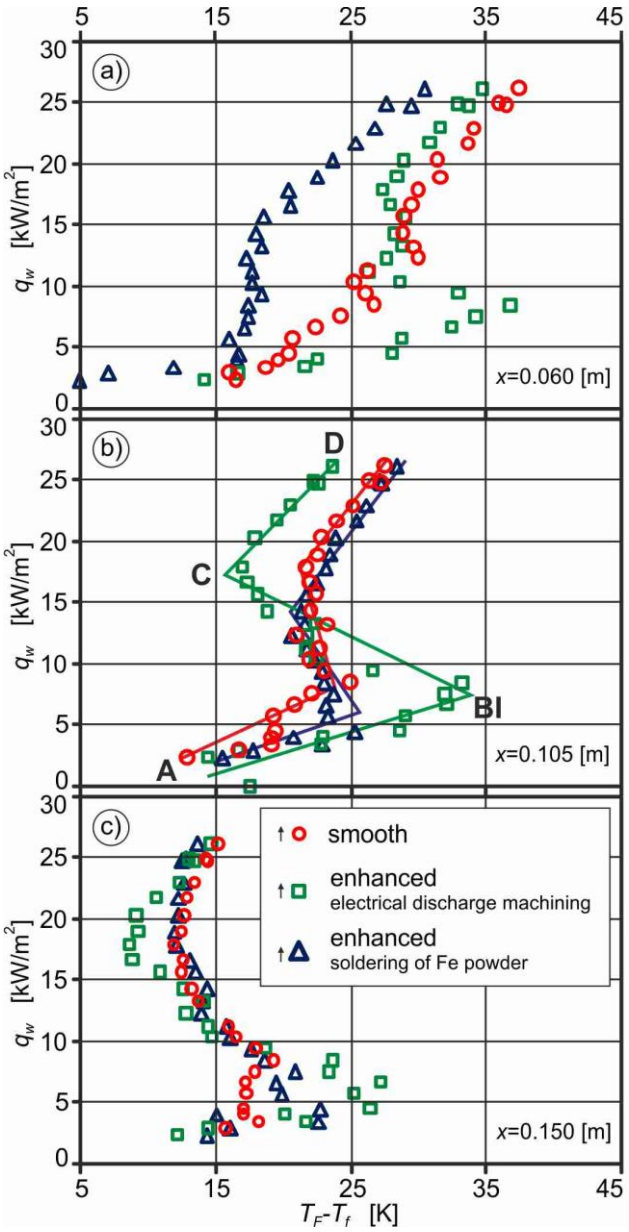

Figure 4 Boiling curves generated for three distances from the minichannel inlet: a) 0.060 m, b) 0.105 m, c) 0.150 m

The experimental results shown in Fig. 4 as boiling curves can be summarized as follows:

- The boiling curves plotted for the smooth heated foil (marked in red) and the foil with soldered iron powder (marked in blue) were similar for the distances 0.105 m and 0.150 m from the minichannel inlet (Fig. 4a,b). In both cases, there was a small drop in temperature in the "nucleation hysteresis".
- From the boiling curves generated for the surface with cavities produced by electrical discharge machining it is

clear that higher differences in temperature T_F-T_f (superheating) occurred at the boiling incipience for three selected distances.

- The boiling curves obtained for the smooth surface and the surface obtained by soldering iron powder (Fig. 4b) were similar in shape in the saturated boiling region.
- The boiling curves drawn for the smooth surface and the surface enhanced by soldering iron powder differed in shape (no nucleation-associated hysteresis) when the distance from the minichannel inlet was 0.060 m.

From the data obtained at distances of 0.105 m and 0.15 m from the minichannel inlet it is evident that the main parts of the boiling curves presented in Fig. 4 are similar. The boiling curves plotted for a distance of 0.06 m from the minichannel inlet differ, which indicates that the influence of the heated surface roughness is the largest in this area. There are differences between the boiling curves in the region of transition from subcooled to saturated boiling and in the fully developed nucleate boiling region. For the surface enhanced by electrical discharge machining the drop in temperature attributable to "nucleation hysteresis" was higher than those reported for the smooth surface and the surface enhanced by soldering iron powder. Furthermore, in the fully developed nucleate boiling region, there were smaller differences in temperature T_F-T_f during high heat flux boiling (sections C-D, Fig. 4b). Moreover, no significant differences in shape were observed between the boiling curves plotted for the smooth surface and the surface enhanced by soldering iron powder.

CONCLUSION

This paper has dealt with results concerning flow boiling heat transfer in three parallel vertically oriented asymmetrically heated rectangular minichannels. A thin alloy foil was used to act as the heated wall for Fluorinert FC-72 flowing in the minichannels. Changes in the temperature on the outer smooth side of the foil were observed with an infrared camera. In one minichannel the surface in contact with the fluid was smooth. In the other two, it was rough. Two types of surface enhancement were analyzed: a surface with unevenly distributed minicavities produced by electrical discharge machining and a surface with a layer of soldered iron powder.

The results were presented as relationships between the heat transfer coefficient and the distance along the minichannel length and as boiling curves. Local values of the heat transfer coefficient were calculated using a one-dimensional method. The experimental data obtained for the two types of enhanced heated surfaces was compared with that recorded for the smooth surface.

In the subcooled boiling region, the heat transfer coefficient was relatively low. The values increased slightly with the distance from the minichannel inlet. In the saturated boiling region, the heat transfer coefficient was very high (with values up to a hundred times higher than those reported for the subcooled boiling region). Local values of the coefficient decreased along the minichannel length. At the highest heat flux, the local values of the heat transfer coefficient obtained for the foil surface enhanced by electrical discharge machining were higher than those reported for the smooth surface or the surface modified by soldering iron powder.

ACKNOWLEDGMENTS

The research reported herein was supported by a grant from the National Science Centre (No. DEC-2013/09/B/ST8/02825).

REFERENCES

[1] Saisorn S., Kaew-On J. and Wongwises S., An experimental investigation of flow boiling heat transfer of R-134a in horizontal and vertical mini-channels, *Experimental Thermal and Fluid Science*, Vol. 46, 2013, pp. 232–244

[2] Kandlikar S.G. and Grande W.J., Evolution of microchannel flow passages-thermohydraulic performance and fabrication technology, *Heat Transfer Engineering*, Vol. 25, 2002, pp. 3–17

[3] Bohdal T., Charun H. and Sikora M., Comparative investigations of the condensation of R134a and R404A refrigerants in pipe minichannels, *International Journal of Heat and Mass Transfer*, Vol. 54, 2011, pp. 1963–1974

[4] Kuczyński W., Charun H. and Bohdal T., Influence of hydrodynamic instability on the heat transfer coefficient during condensation of R134a and R404A refrigerants in pipe mini-channels, *International Journal of Heat and Mass Transfer*, Vol. 55(4), 2012, pp. 1083–1094

[5] Kanizawa F. T., Tibiriçá C. B. and Ribatski G., Heat transfer during convective boiling inside microchannels, *International Journal of Heat and Mass Transfer*, Vol. 93, 2016, pp. 566–583

[6] Dutkowski K., Two-phase pressure drop of air–water in minichannels, *International Journal of Heat and Mass Transfer*, Vol. 52, 2009, pp. 5185–5192

[7] Dutkowski K., Influence of the flashing phenomenon on the boiling curve of refrigerant R134a in minichannels, *International Journal of Heat and Mass Transfer*, Vol. 53, 2010, pp. 1036–1043

[8] Mikielewicz D., A new method for determination of flow boiling heat transfer coefficient in conventional-diameter channels and minichannels, *Heat Transfer Engineering*, Vol. 31, 2010, pp. 276–287

[9] Mikielewicz D. and Mikielewicz J., A common method for calculation of flow boiling and flow condensation heat transfer coefficients in minichannels with account of nonadiabatic effects, *Heat Transfer Engineering*, Vol. 32, 2011, pp. 1173–1181

[10] Ozer A.B., Oncel A.F, Hollingsworth D.K. and Witte L.C., A method of concurrent thermographic–photographic visualization of flow boiling in a minichannel, *Experimental Thermal and Fluid Science*, Vol. 35, 2011, pp. 1522–1529

[11] Jokar A., Hosni M. H. and Eckels S. J., Correlations for heat transfer and pressure drop of glycol-water and air flows in minichannel heat exchangers, *ASHRAE Transaction*, Vol. 111 PART 2(2), 2005, pp. 213–224

[12] Cieśliński J. T., Flow and pool boiling on porous coated surfaces, *Reviews in Chemical Engineering*, Vol. 27(3-4), 2011, pp. 179–190

[13] Ammerman C.N. and You S.M., Enhancing Small-Channel Convective Boiling Performance Using a Microporous Surface Coating, *Journal of Heat Transfer*, Vol. 123(5), 2001, pp. 976–983

[14] Jones B. J. and Garimella S. V., Surface Roughness Effects on Flow Boiling in Microchannels, *Journal of Thermal Science and Engineering Applications*, Vol. 1(4), 2009, pp. 041007-1–9

[15] Piasecka M., Heat transfer research on enhanced heating surfaces in flow boiling in a minichannel and pool boiling, *Annals of Nuclear Energy*, Vol. 73, 2014, pp. 282–293

[16] Hożejowska S., Homotopy Perturbation Method Combined with Trefftz Method in Numerical Identification of Temperature Fields in Flow Boiling, *Journal of Theoretical and Applied Mechanics*, Vol. 53(4), 2015, pp. 969–980
[17] Piasecka M., Correlations for flow boiling heat transfer in minichannels with various orientations, *International Journal of Heat and Mass Transfer*, Vol. 81, 2014, pp. 114–121
[18] Piasecka M., Strąk K. and Maciejewska B., Calculations of Flow Boiling Heat Transfer in a Minichannel based on Liquid Crystal and Infrared Thermography, *Heat Transfer Engineering*, Vol. 38(1), 2017 (in print)
[19] Piasecka M., Impact of selected parameters on refrigerant flow boiling heat transfer and pressure drop in minichannels, *International Journal of Refrigeration*, 2015, Vol. 56, pp. 198–212
[20] Piasecka M. and Maciejewska B., Heat transfer coefficient during flow boiling in a minichannel at variable spatial orientation, *Experimental Thermal and Fluid Science*, 2015, vol. 68, pp. 459–467
[21] Piasecka M., Laser Texturing, Spark Erosion and Sanding of the Surfaces and their Practical Applications in Heat Exchange Devices, *Advanced Materials Research*, Vol. 874, 2014, pp. 95–100
[22] Hożejowska S., Maciejewska B. and Poniewski M.E., Numerical Analysis of Boiling Two-Phase Flow in Mini- and Microchannels, *Encyclopedia of Two-Phase Heat Transfer and Flow I. Fundamentals and Method*, 2015, World Scientific Publishing Co Ltd, New Jersey
[23] Passos J.C., Hirata F.R., Possamai L.F. B., Balsamo M. and Misale M., Confined boiling of FC72 and FC87 on a downward facing heating copper disk, *International Journal of Heat and Fluid Flow*, Vol. 25(2), 2004, pp. 313–319
[24] Bi Q., Zhao T., Guo Y. and Chen T., Experimental Investigations on Boiling Heat Transfer Inside Miniature Circular Tubes Immersed in FC-72, *Journal of Thermal Science*, Vol. 11(4), 2002, pp. 303-307
[25] Auracher H. and Buchholz M., Experiments on the fundamental mechanisms of boiling heat transfer, *Journal of the Brazilian Society of Mechanical Sciences and Engineering*, Vol. 27(1), 2005, pp. 1–22
[26] Grassi W. and Testi D., Heat transfer enhancement by electric fields in several heat exchange regimes, *Annals of the New York Academy of Sciences*, Vol. 1077, 2006, pp. 527–569
[27] Orzechowski T., Heat transfer on ribs with microstructured surface (in Polish), *Monographs, studies, hearings, 39*, 2013, Kielce University of Technology
[28] Piasecka M., Determination of the Temperature Field Using Liquid Crystal Thermography and Analysis of Two-Phase Flow Structures in Research on Boiling Heat Transfer in a Minichannel, *Metrology and Measurement Systems*, Vol. 20(2), 2013, pp. 205–216
[29] Piasecka M. and Maciejewska B., The study of boiling heat transfer in vertically and horizontally oriented rectangular minichannels and the solution to the inverse heat transfer problem with the use of the Beck method and Trefftz functions, *Experimental Thermal and Fluid Science*, Vol. 38, 2012, pp. 19–32
[30] Celata G. P., Saha S. K., Zummo G. and Dossevi D., Heat transfer characteristics of flow boiling in a single horizontal microchannel, *International Journal Thermal Sciences*, Vol. 49, 2010, pp. 1086–1094
[31] Piasecka M., Michalski D. and Strąk K., Comparison of two methods for contactless surface temperature measurement, *EPJ Web of Conferences*,Vol. 114, 2016, paper No. 02094.
[32] Kaniowski R., Piasecka M. and Poniewski M. E., Flow boiling in minichannels, *Encyclopedia of two-phase heat transfer and flow I. Fundamentals and Methods. Special Topics in Pool and Flow Boiling*, 2015, pp. 75–105
[33] Bohdal T., Development of bubbly boiling in channel flow, E*xperimental Heat Transfer*, Vol. 4, 2001, pp. 199–215